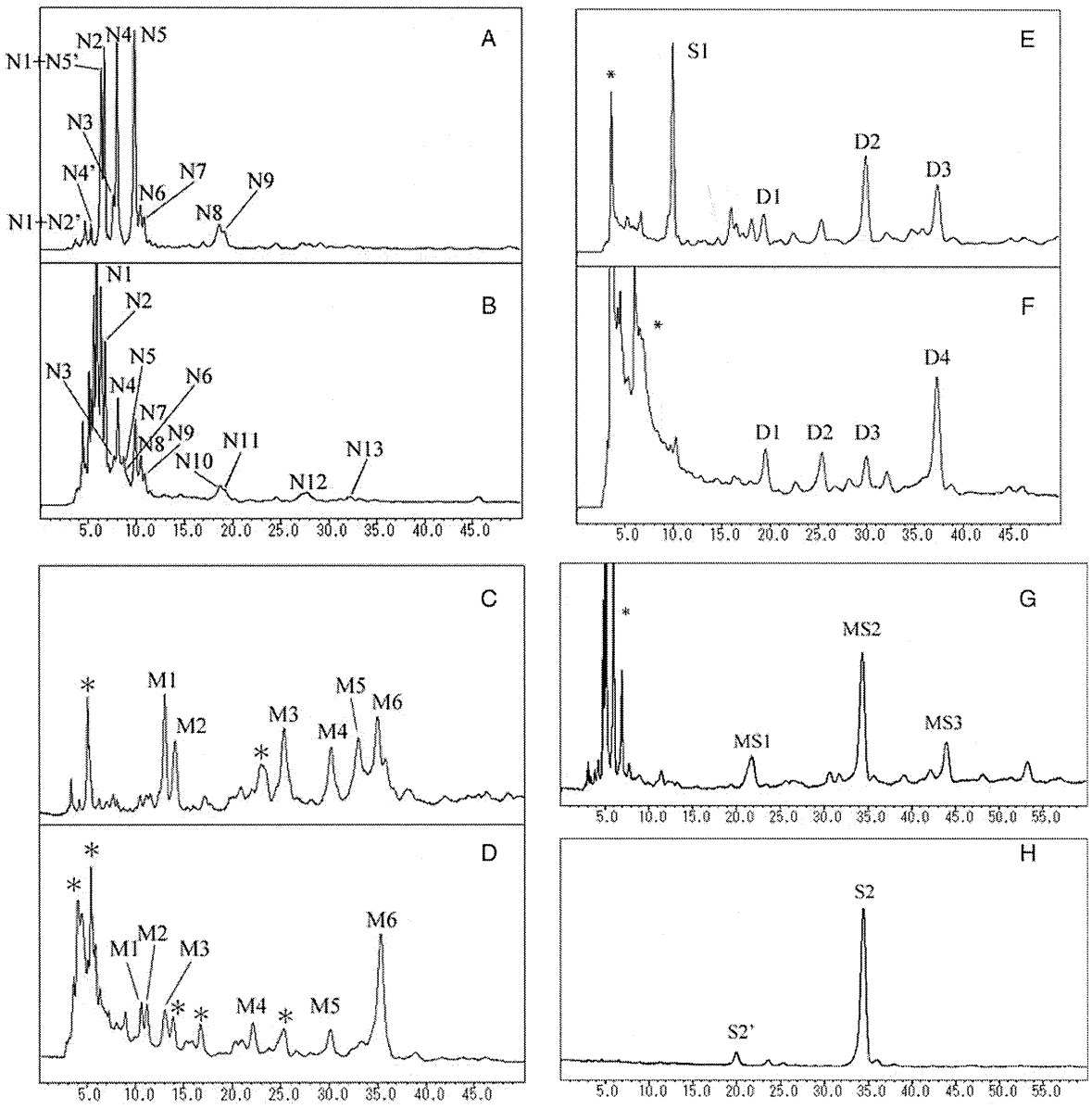

Fig. 2. Reverse-phase ODS elution profiles of PA-glycans obtained from each different fraction separated on the DEAE column. The neutral, mono-sialyl, di-sialyl or mono-sulfate, mono-sialyl-mono-sulfate and di-sulfate fractions were individually applied to the ODS column and gave elution profiles according to their hydrophobicity. (**A**) pig Peak 1, (**B**) human Peak 1, (**C**) pig Peak 2, (**D**) human Peak 2, (**E**) pig Peak 3, (**F**) human Peak 3, (**G**) pig Peak 4 and (**H**) pig Peak 5. N2′: Epimerization of N2; N4′: Epimerization of N4; N5′: Epimerization of N5; S2′: Epimerization of S2. Asterisks indicate the fractions containing no detectable PA-oligosaccharides.

as well. Among them, one neutral, five mono-sialyl and six sulfates of *N*-linked glycans in the API preparation were not detected in human islets. The structures of 9 of these 12 glycans were clearly identified in this study.

Concerning the characteristics of the *N*-glycans identified in the API preparation, the neutral glycans contained relatively high levels (%) of high-mannose type glycans. In comparison with the *N*-glycans from human islets, the high-mannose type of *N*-glycan found in API contains high levels (5 or 6) of mannoses. In addition, glycans with structures of fractions N6-2 were not detected in human islets. On the other hand, in the case of API, the relative content of sulfated *N*-glycans approached 10%. In addition, the di-sulfate type glycans represented 7% of the relative quantity, indicating that sulfated *N*-glycans are a common structure in *N*-glycans of API but do not appear to be produced by human islets. In addition, all the sulfates are attached to a β-linked *N*-acetylgalactosamine (GalNAc).

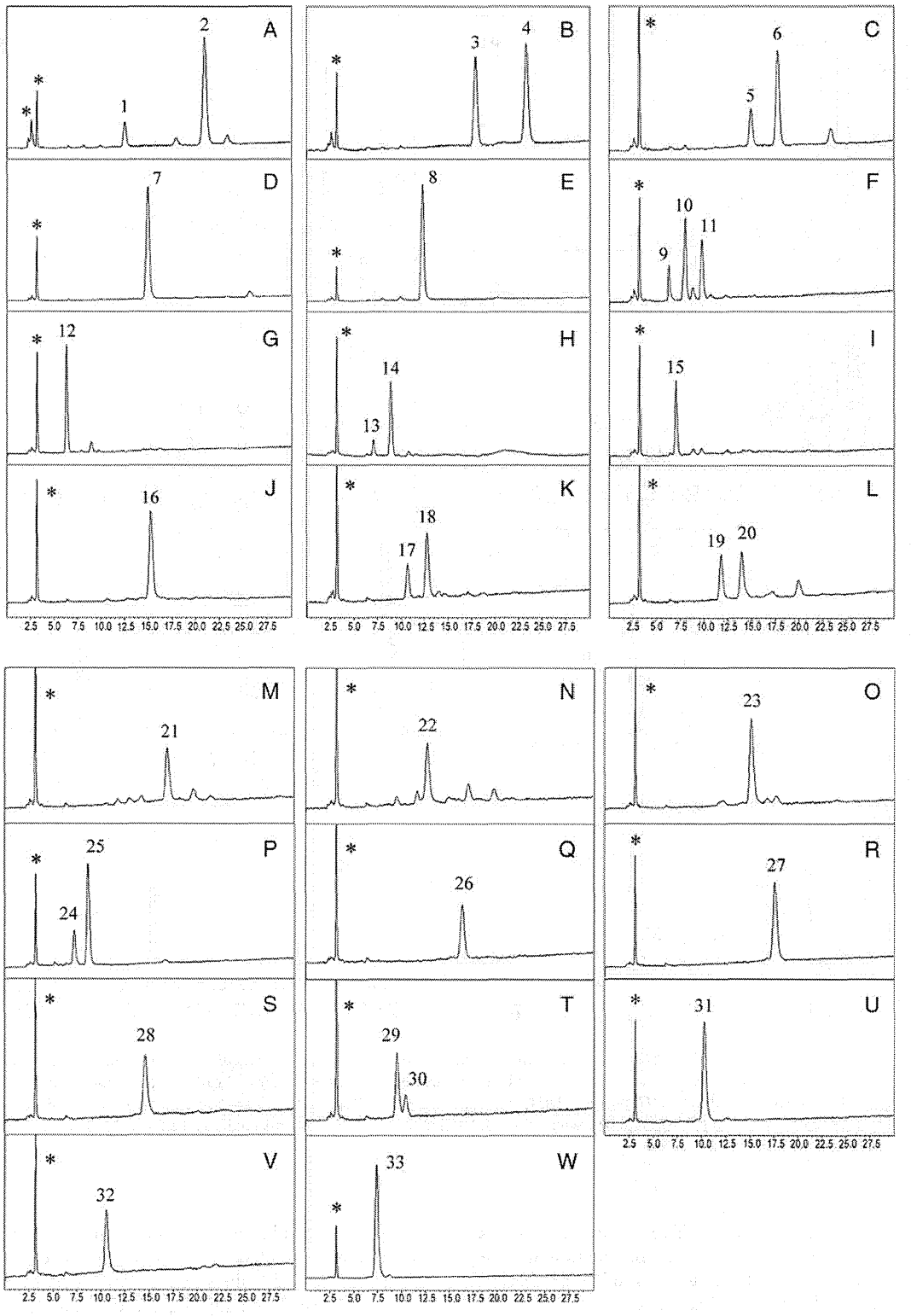

Fig. 3. Amide column elution profiles of PA-glycans of pig islets from each different fraction separated on the ODS column. (**A**) ODS peak-N1 + N5′. Peak 1 is the epimerization of the ODS peak-N5. Peak 2 was then settled as N1. (**B**) ODS peak-N2. Peaks 3 and 4 correspond to N2-1 and N2-2, respectively. (**C**) ODS peak-N3. Peak 5 was contamination of the ODS peak-N4. Peak 6 corresponds to N3. (**D**) ODS peak-N4. Peak 7 corresponds to N4. (**E**) ODS peak-N5. Peak 8 corresponds to N5. (**F**) ODS peak-N6. Peak 9 was contamination of ODS peak-N7. Peaks 10 and 11 correspond to N6-1 and N6-2, respectively. (**G**) ODS peak-N7. Peak 12 corresponds to N7. (**H**) ODS peak-N8. Peak 13 was contamination of ODS peak-N9. Peak 14 corresponds to N8. (**I**) ODS peak-N9. Peak 15 corresponds to N9. (**J**) ODS peak-M1.

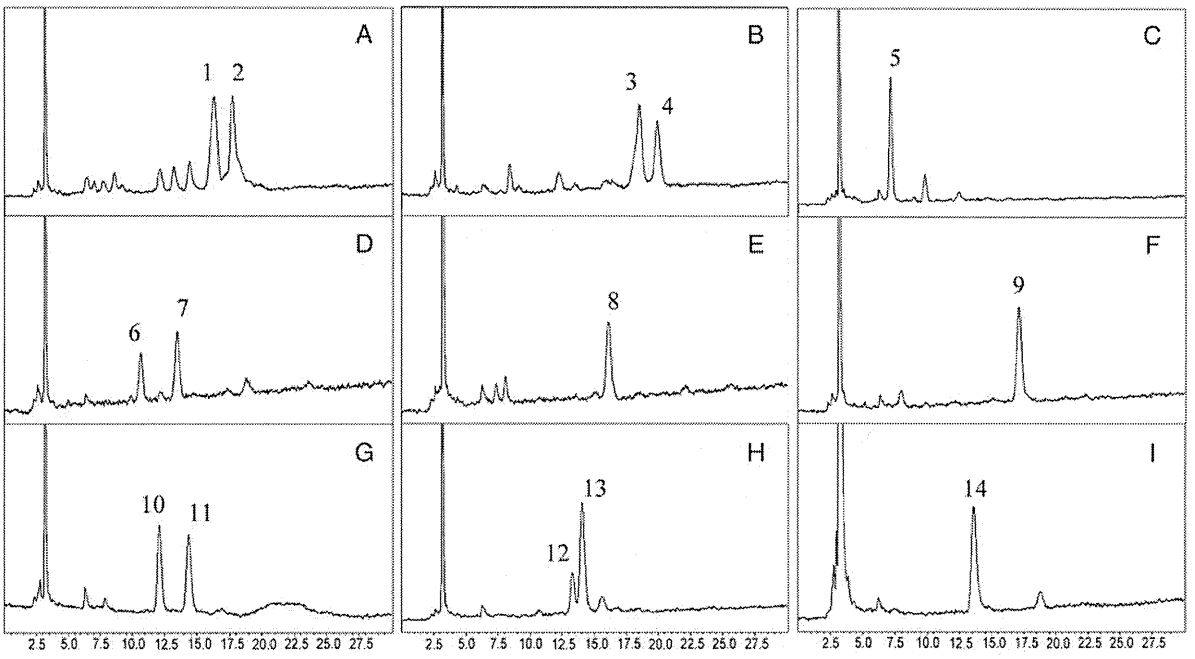

Fig. 4. Amide column elution profiles of PA-glycans from each fraction separated on the ODS column of human islets. (**A**) ODS peak-N5. Peaks 1 and 2 correspond to N5-1 and N5-2, respectively. (**B**) ODS peak-N6. Peaks 3 and 4 correspond to N6-1 and N6-2, respectively. (**C**) ODS peak-N11. Peak 5 corresponds to N11. (**D**) ODS peak-N12. Peaks 6 and 7 correspond to N12-1 and N12-2, respectively. (**E**) ODS peak-N13. Peak 8 corresponds to N13. (**F**) ODS peak-M1. Peak 9 corresponds to M1. (**G**) ODS peak-M2. Peaks 10 and 11 correspond to M2-1 and M2-2, respectively. (**H**) ODS peak-M4. Peaks 12 and 13 correspond to M4-1 and M4-2, respectively. (**I**) ODS peak-D2. Peak 14 corresponds to D2.

No terminal fucose was detected in the *N*-glycans from either type of islets in this study.

Previous studies reported by other groups concluded that many kinds of *N*-glycans are found in API, using MALDI-TOF/MS and MS/MS (Kim, Gil et al. 2008; Kim, Gil et al. 2009; Kim, Harvey et al. 2009). The difference in the number of detected *N*-glycans in this study can be attributed to the sensitivity of the MS method and HPLC. It, thus, appears that the accuracy of the data presented here using HPLC mapping in conjunction with a MALDI-TOF technique provided much more detailed information. That is, MS data are sensitive and can be rapidly obtained, but indicate only a glycan structure based on the calculated molecular weight. Therefore, discriminating between isomeric structures becomes difficult (Wheeler and Harvey 2001). In addition, except for N-glycolylneuraminic acid (NeuGc), it does not indicate the specific structure of sialyl acids present. On the other hand, the data reported herein can be used to identify the representative features of each *N*-glycan in the API preparation. However, the possibility that several glycans, such as pN6-2, pM2-1, pM2-2, pM3-1, pM3-2 and pM5, that were not detected in humans islets as major *N*-glycans are expressed in human islets at very low levels cannot be completely excluded. In addition, concerning the sulfated *N*-glycans such as S1-1, S1-2, S2, MS1 and MS3, the accuracy in identifying the position of the SOH3 attached to β1-4GalNAc was not clear in this study, and it is possible that these sulfated glycans also may be produced in human islets or other tissues, because humans produce several sulfotransferase enzymes that can catalyze the attachment of a sulfate to GalNAc (Boregowda et al. 2005).

Chlorate is a selective inhibitor of adenosine triphosphate sulfate adenylyltransferase, the first enzyme in the sulfate activation pathway (Girard et al. 1998). It inhibits all sulfotransferases. Therefore, although API had a diminished antigenicity to human serum, especially IgM, as a result of the presence of sodium chlorate treatment, a structural analysis of the changes on the sulfated *N*-glycans and other nonsulfated glycans of the API after the treatment might be needed to assess antigenicity issues. On the other hand, it was not possible to determine the binding site of the sulfate residue to GalNAc using this method. However, the possibility that the sulfate residue is one of the non-Gal antigens in pig islets cannot be excluded based on the data presented herein. Further study will be needed to analyze the non-Gal antigen in pig islets, especially to sulfotransferase enzymes.

In comparison with a report concerning the pig lung and trachea, using exactly the same HPLC mapping in conjunction with the MALDI-TOF technique, Sriwilaijaroen et al. (2011) reported a relatively small percent of high-mannose type

Peak 16 corresponds to M1. (**K**) ODS peak-M2. Peaks 17 and 18 correspond to M2-1 and M2-2, respectively. (**L**) ODS peak-M3. Peaks 19 and 20 correspond to M3-1 and M3-2, respectively. (**M**) ODS peak-M4. Peak 21 corresponds to M4. **N**: ODS peak-M5. Peak 22 corresponds to M5. (**O**) ODS peak-M6. Peak 23 corresponds to M6. (**P**) ODS peak-S1. Peaks 24 and 25 were identified as S1-1 and S1-2, respectively. (**Q**): ODS peak-D1. Peak 26 corresponds to D1. (**R**) ODS peak-D2. Peak 27 corresponds to D2. (**S**) ODS peak-D3. Peak 28 corresponds to D3. (**T**) ODS peak-MS1. Peak 29 corresponds to MS1. Peak 30 is the epimerization of ODS peak-MS2. (**U**) ODS peak-MS2. Peak 31 corresponds to MS2. (**V**) ODS peak-MS3. Peak 32 corresponds to MS3. (**W**) ODS peak-S2. Peak 33 corresponds to S2. *Not a sugar.

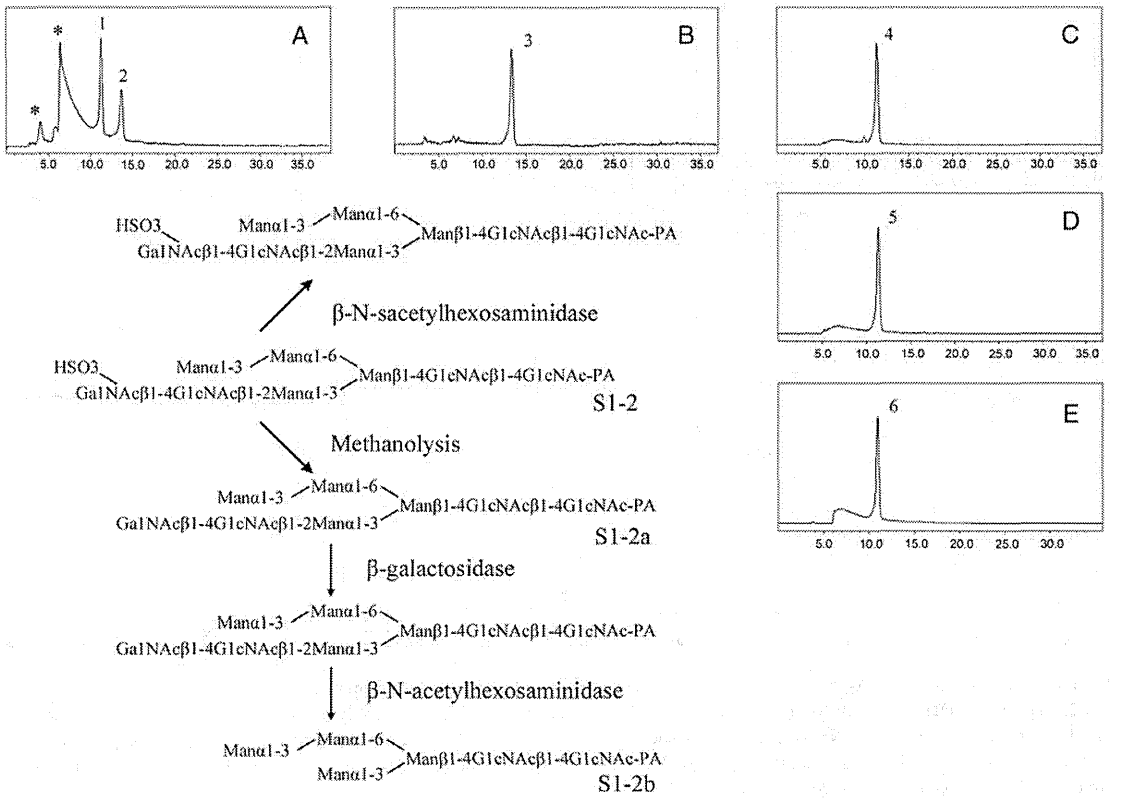

Fig. 5. Structural analysis of S1-2. (**A**) ODS peak after methanolysis treatment of S1-2. Peak 1 is the nonreacted sample, S1-2 (7.5 GU and 1641 Da). Peak 2 corresponds to S1-2a (8.3 GU and 1557 Da). (**B**) ODS peak after β-galactosidase treatment to S1-2a. Peak 3 is identical to S1-2a in ODS (GU) and molecular weight. (**C**) ODS peak after β-*N*-acetylhexosaminidase treatment of S1-2a. Peak 4 corresponds to S1-2b (7.5 GU and 1151 Da). (**D**) ODS peak after co-chromatography of S1-2b and M4.1. S1-2b was then proved to be the same structure as M4.1 in GALAXY. (**E**) ODS peak after β-galactosidase treatment to S1-2. Peak 6 is just the same as S1-2 in GU and molecular weight. * Not a sugar.

N-glycans. However, in this study, pig islets contain a relatively large percent of *N*-glycans, 81%, and human islets also contain 76.7%. Therefore, this evidence related to high-mannose types was assumed to be a typical feature of islets. It is noteworthy that in this pig islets study no evidence was found for the presence of α-Gal and NeuGc structures, while the pig lung and trachea clearly produce both antigens. Concerning α-Gal, as has been indicated in many reports, pig islets express very low levels of α-Gal. On the other hand, concerning NeuGc, our previous study reported that NeuGc is expressed on the *N*-glycans of API (Komoda et al. 2004). Therefore, pig islets must contain NeuGc in relatively minor amounts and, as a result, were not detected in this study, because pig lung and trachea contain relatively minor levels of NeuGc structures.

In addition, NeuGc-Gal-GlcNAc and Galα1-3 Lewis x (Lew^x) were recently reported as novel antigens, as evidenced by a structural analysis of *N*-glycans from the miniature pig kidney (Kim et al. 2006). However, neither of these antigens was detected in this study.

Blixt et al. (2009) reported on the carbohydrate specificities of sera obtained from clinical patients in whom neonatal bone pig islet-like cell clusters (NPCC) had been intraportally injected, using a printed covalent glycan array with 200 structurally defined glycans. Besides α-Gal and NeuGc, the patients had Abs against terminal α-linked GalNAc, β3-linked Gal especially Galβ1,3GlcNAc even if terminally sulfated or sialylated, β-GlcNAc except for β1,3-linked, oligomannosyl compounds, some neuranimic acid (NeuAc) and Galα1-3Lew^x. Compared with the data reported here, pM5 has β-GlcNAc, might be applicable for the target structure of the patients. In addition, N6-2, pM2-2 and pM3-2, which contain Manα1-3Manα1-6Man structures, are also potential target antigens. However, the antigenicity of NPCC may slightly be different from that for API.

As the other non-Gal antigens, the Forssman, the terminal GalNAc related to the Tn-antigen (GalNAcα-*O*-Ser/Thr), T-antigen (Thomsen-Friedenreich; Galβ1,3GalNAcα-*O*-Ser/Thr) and sialyl-Tn antigen (NeuAcα2,6GalNAcα-*O*-Ser/Thr) are also reported to be important (Ezzelarab et al. 2005). However, these glycans are related to *O*-glycans and glicolipids (Diswall et al. 2011).

In summary, as a feature, pig islets are rich in high-mannose type *N*-glycans, especially relatively low amounts of mannose. Several API structures, such as N6-2, pM2-1, 2-2, 3-1, 3-2, and pM5, and the sulfate structure, β-linked GalNAc-SOH3, were not detected in human islets. In addition, it is possible that the sulfated glycans of API are involved in the observed antigenicity to human serum. The data herein provide important information that can be useful to future clinical xenotransplantation studies.

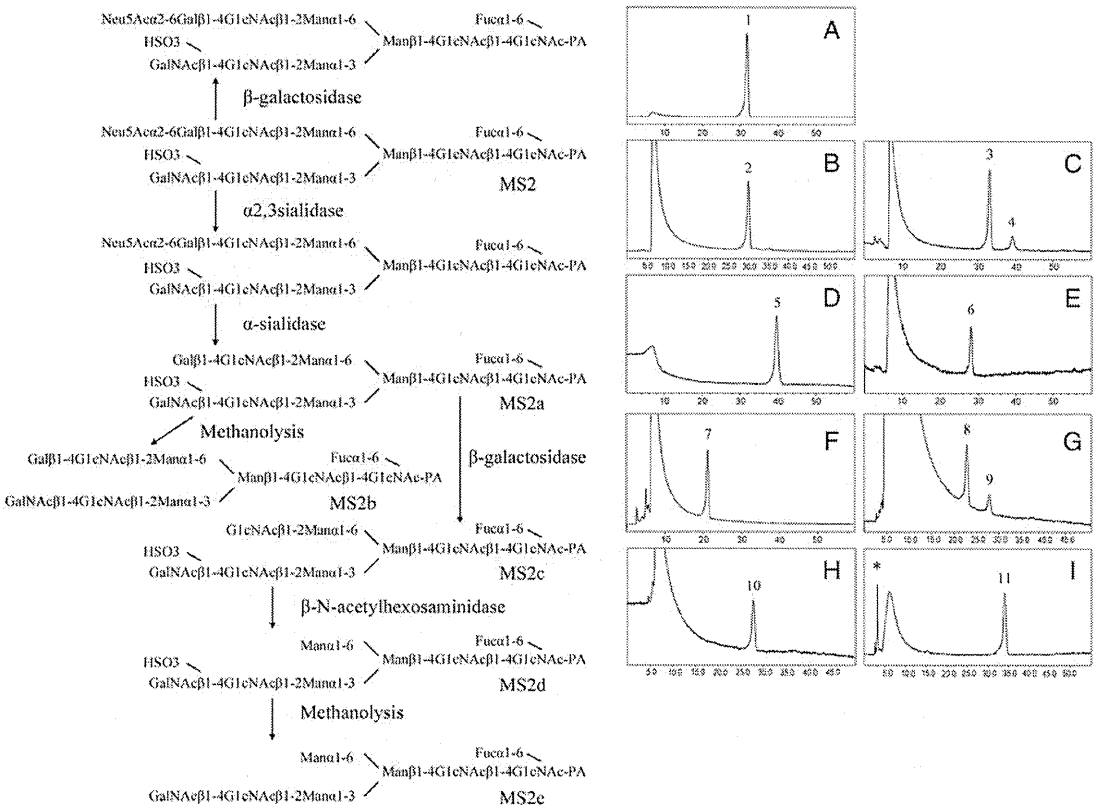

Fig. 6. Structural analysis of MS2. (**A**) ODS peak after α2,3-sialidase treatment to MS2. Peak 1 was just the same as MS2 in GU and molecular weight. (**B**) ODS peak after α-sialidase treatment to MS2. Peak 2 corresponds to MS2a (12.1 GU and 1988 Da). (**C**) ODS peak after methanolysis treatment to MS2a. Peak 3 is the nonreacted sample. Peak 4 lacked one sulfate residue from MS2a and corresponds to MS2b (13.9 GU and 1907 Da). (**D**) ODS peak after co-chromatography of MS2b and 210.4a in GALAXY. MS2b was proved to be the same structure as the 210.4a in GALAXY. (**E**) ODS peak after β-galactisidase treatment to MS2a. Peak 6 lacked one galactose from MS2a and corresponds to MS2c (11.4 GU and 1826 Da). (**F**) ODS peak after β-*N*-acetylhexosaminidase treatment to MS2c. Peak 7 corresponds to MS2d (9.7 GU and 1622 Da). (**G**) ODS peak after methanolysis treatment of MS2d. Peak 8 was the nonreacted sample. Peak 9 lacked one sulfate residue from MS2d and corresponds to MS2e (11.0 GU and 1541 Da). (**H**) ODS peak after co-chromatography of MS2e and 110.4a in GALAXY. MS2e was proved to be the same structure as the 110.4a in GALAXY. (**I**) ODS peak after β-galactisidase treatment to MS2. Peak 11 is identical to MS2 in GU and molecular weight. * Not a sugar.

Materials and methods

Pig islet isolation

Pancreatic glands were removed from several pigs at a slaughterhouse that handles young market weight pigs (Large White/Landrace x Duroc, 6 months old, ~100 kg). Isolation of porcine islets was performed using the Islet Isolation Technique (Goto et al. 2004), with minor modifications. Purified islet fractions were pooled and cultured at 37°C in a humidified atmosphere with 5% CO_2 in CMRL1066 medium (Biochrom, Berlin, Germany) supplemented with 20% heat inactivated porcine serum, 2 mm *N*-acetyl-L-alanyl-L-glutamine, 10 mM *N*-2-hydroxyethylpiperazine-*N*1-2-ethanesulfonic acid, 100 IU/mL penicillin, 100 μg/mL streptomycin (Biochrom) and 20 μg/mL ciprofloxacin (Bayer, Leverkusen, Germany).

Human islet isolation

The method used to isolate islets has been reported previously (Matsumoto et al. 2002). In brief, the pancreas was distended with a cold enzyme solution through the pancreatic duct using a pressure-controlled pump system. In all cases, the distended pancreata were digested using the semi-automated method (Matsumoto et al. 2006). All centrifuged pellets were collected in cold storage/purification stock solution (Mediatech, Inc., Manassas, VA).

Islet isolations were conducted based on the Edmonton protocol with our modifications. The results of the isolations were evaluated based on the Edmonton protocol. Islets were purified with a COBE 2991 cell processor (CaridianBCT, Inc., Lakewood, CO) using density-adjusted iodixanol-based continuous density gradient. The final preparation of islets was assessed using dithizone staining (Sigma Chemical Co., St. Louis, MO) for islet yield and purity. Islet yield was converted into a standard number of islet equivalents (diameter standardizing to 150 μm). Islet viability was evaluated with fluorescein diacetate (10 μmol/L) and propidium iodide (15 μmol/L) staining. All procedures were done at the Baylor Research Institute, TX.

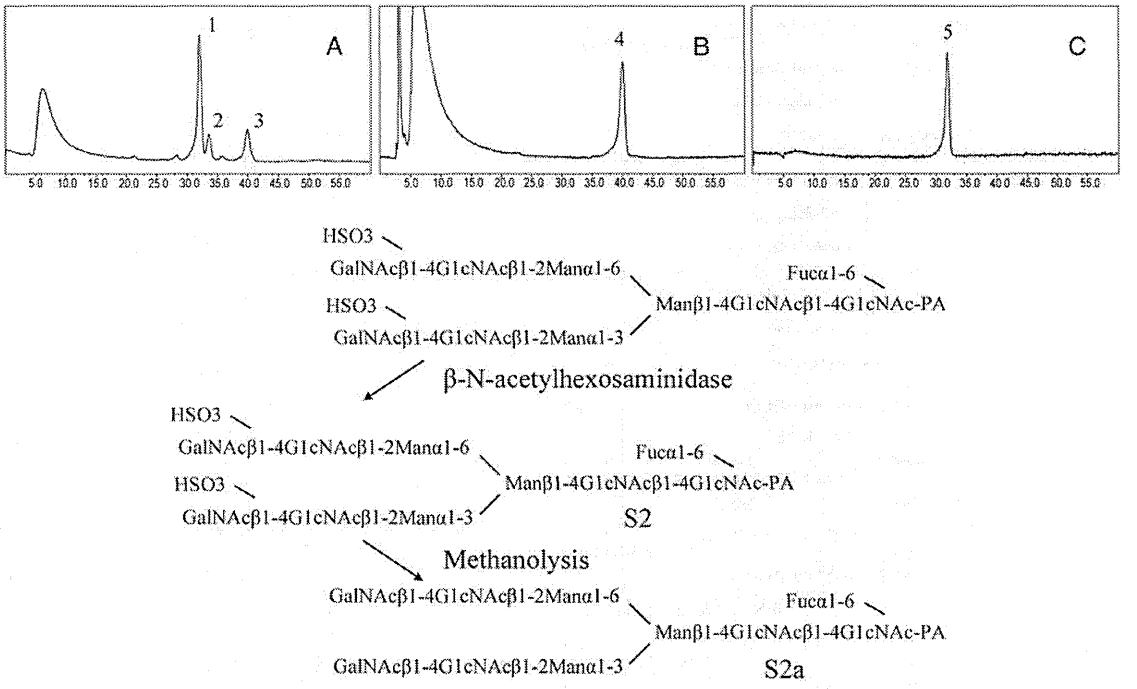

Fig. 7. Structural analysis of S2. (**A**) ODS peak after methanolysis treatment to S2. Peak 1 was the nonreacted sample, S2 (12.7 GU, 2110 Da). Peak 2 lacked one sulfate residue from S2, 13.2 GU and 2029 Da. Peak 2 lacked two sulfate residues from S2, corresponding to S2a (15.1 GU and 1948 Da). (**B**) ODS peak after co-chromatography of the samples of S2a and210.4b. S2a was the same structure as the 210.4b in GALAXY. (**C**) ODS peak after β-*N*-acetylhexosaminidase treatment of S2. Peak 5 was identical to S2 in GU and molecular weight.

Materials for analyses

Glycoamidase A from sweet almond, α-manosidase, β-galactosidase and β-*N*-acetylhexosaminidase from jack bean were purchased from Seikagaku Kogyo Co. (Tokyo, Japan). α-Gal from coffee bean was purchased from Oxford GlycoSciences, Inc. (Oxford, UK). Trypsin and chymotrypsin were obtained from Sigma (St. Louis, MO). Pronase protease from *Streptomyces griseus* was from Calbiochem (San Diego, CA). The PA derivatives of isomalto-oligosaccharides 4–20 (indicating the degree of polymerization of glucose residues) and reference PA-oligosaccharides were purchased from Seikagaku Kogyo Co.

Characterization of N-glycan derived from islets

The residue after extracting each islet with a chloroform–methanol solution was used as the starting material. All experimental procedures used, including the chromatographic conditions and glycosidase treatments, have been described previously (Takahashi et al. 2001). The extract was proteolyzed with chymotrypsin and trypsin mixture and further digested with glycoamidase A to release *N*-glycans. After the removal of the peptide materials, the reducing ends of the *N*-glycans were derivatized with 2-aminopyridine (Wako, Osaka, Japan). This mixture was applied to a DEAE column (Tosoh, Tokyo, Japan) or a TSK-gel Amide-80 column (Tosoh), and each fraction that was separated on the amide column was applied to a Shim-pack HRC-ODS column (Shimadzu, Kyoto, Japan). The elution times of the individual peaks onto the amide-silica and ODS columns were normalized with respect to a PA-derivatized isomalto-oligosaccharide with a known degree of polymerization, and are represented in units of glucose unit (GU). Thus, a given compound from these two columns provided a unique set of GU values, which corresponded to the coordinates of the two dimension HPLC map. The PA-oligosaccharides were identified by comparison with the coordinates of <500 reference PA-oligosaccharides in a homemade web application, GALAXY (http://www.glycoanalysis.info/) (Takahashi and Kato 2003). The calculated HPLC map based on the unit contribution values was used to estimate some high-mannose type PA-oligosaccharides. The PA-oligosaccharides were co-chromatographed with the reference to PA-oligosaccharides on the columns to confirm their identities.

MS analyses of PA-glycans

PA-oligosaccharides were subjected to MALDI-TOF-MS analysis. The matrix solution was prepared as follows: 10 mg of 2,5-dihydroxybenzoic acid (Sigma) was dissolved in 1:1 (v/v) of acetonitrile/water (1 mL). Stock solutions of PA-glycans were prepared by dissolving them in pure water. One microliter of sample solution was mixed on the target spot of a plate with 1 μL of matrix solution and then allowed to air-dry. MALDI-TOF-MS data were acquired in the positive modes using AXIMA-CFR (Shimadzu) operated in the linear mode.

Single islet cell preparation

Single-cell suspensions were prepared by the method described by Ono et al. (1977). Isolated islets were exposed to 0.04% ethylenediaminetetraacetic acid for 5 min at room temperature

Table I. Structures and relative quantities of neutral, mono-sialyl, di-sialyl or mono-sulfate, mono-sialyl-mono-sulfate and di-sulfate PA-oligosaccharides derived from human and porcine islets

Peak code number	GU[a] ODS (Amid)	Molecular[b] mass (Da)	Structure[c]	Relative quantity (%)[d]	
				Pig	
Neutral glycan					
N1	4.9 (8.8)	1800	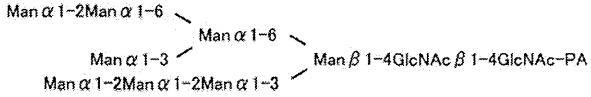	11.6	24.9
N2-1	5.3 (7.9)	1638	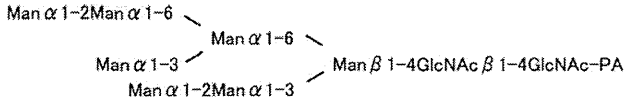	5.8	3.5
N2-2	5.3 (9.5)	1962	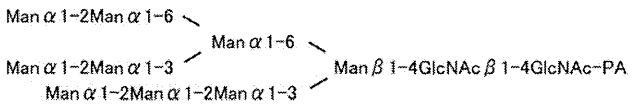	7.4	9.5
N3	6.0 (7.9)	1638	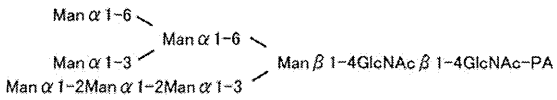	3.0	1.9
N4	6.2 (7.0)	1475	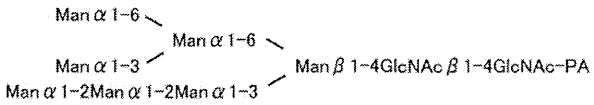	16.7	10.1
pN5 = hN7	7.3 (6.1)	1313	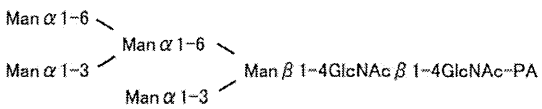	24.0	11.3
pN6-1 = hN8	7.5 (4.2)	989	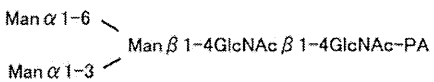	2.3	6.2

Continued

Table I. (Continued)

Peak code number	GU[a] ODS (Amid)	Molecular[b] mass (Da)	Structure[c]	Relative quantity (%)[d]	
				Pig	
pN6-2	7.5 (5.1)	1151	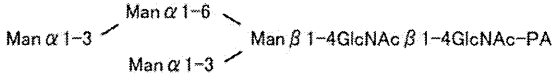	1.7	-
pN7 = hN9	7.7 (3.3)	827	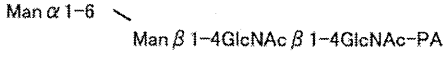	2.4	2.2
pN8 = hN10	10.3 (4.6)	1135	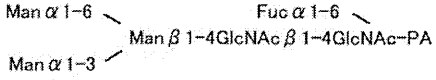	3.9	4.1
pN9 = hN11	10.5 (3.7)	973	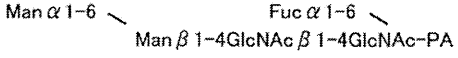	2.2	3.0
hN12-1	12.8 (5.4)	1541	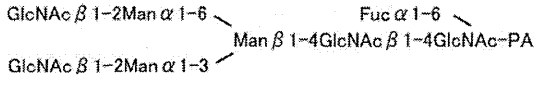	–	1.8
hN12-2	12.8 (6.5)	1948	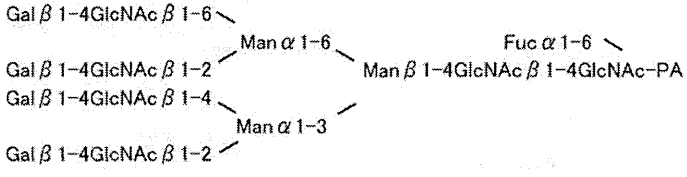	–	2.9
hN13	14.2 (7.4)	1866	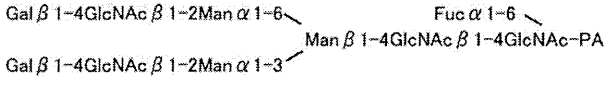	–	3.1
hN5-1	6.6 (7.4)	1558	(Hexose)4(HexNAc)4(PA)1[e]	–	2.7
hN5-2	6.6 (7.9)	1720	(Hexose)5(HexNAc)4(PA)1[e]	–	2.0
hN6-1	6.9 (8.1)	1720	(Hexose)5(HexNAc)4(PA)1[e]	–	1.5
hN6-2	6.9 (8.5)	1882	(Hexose)6(HexNAc)4(PA)1[e]	–	1.2

[a]Units of GU were calculated from the elution times of the peaks obtained from the ODS column in Figure 2 and the Amide column in Figure 3.
[b]Average mass calculated from the *m/z* values of $[M+Na]^+$ or $[M+H]^+$ ion for neural, $[M-H]^-$ ion for mono-sialyl and mono-sulfated and $[M+Na-2H]^-$ ions for mono-sialyl-mono-sulfated and di-sulfated PA-oligosaccharides (Supplementary data, Figure S1).
[c]Structures of PA-oligosaccharides are represented.
[d]Molecular percentage of was calculated from the peak area in Figure 2 by comparison with total *N*-glycan content in each islet tissue.
[e]*N*-glycans did not coincide with those of known references in the GALAXY database.

Table II. Structures and relative quantities of neutral, mono-sialyl, di-sialyl or mono-sulfate, mono-sialyl-mono-sulfate and di-sulfate PA-oligosaccharides derived from human and porcine islets

Peak code number	GU[a] ODS (Amid)	Molecular[b] mass (Da)	Structure[c]	Relative quantity (%)[d]	
				Pig	Human
Mono-sialyl glycan					
pM2-1	9.0 (5.4)	1646	Man α 1-6 \ Man β 1-4GlcNAc β 1-4GlcNAc-PA / Neu5Ac α 2-3Gal β 1-4GlcNAc β 1-2Man α 1-3	0.2	–
pM3-1	11.9 (5.9)	1792	Man α 1-6 \ Fuc α 1-6 \ Man β 1-4GlcNAc β 1-4GlcNAc-PA / Neu5Ac α 2-3Gal β 1-4GlcNAc β 1-2Man α 1-3	0.3	–
hM2-1	7.9 (6.0)	1646	Man α 1-6 \ Man β 1-4GlcNAc β 1-4GlcNAc-PA / Neu5Ac α 2-6Gal β 1-4GlcNAc β 1-2Man α 1-3	–	0.15
pM1 = hM3	8.6 (7.1)	1970	Man α 1-6 \ Man α 1-6 \ Man α 1-3 / Man β 1-4GlcNAc β 1-4GlcNAc-PA / Neu5Ac α 2-3Gal β 1-4GlcNAc β 1-2Man α 1-3	0.6	0.2
pM2-2	9.0 (6.2)	1808	Man α 1-6 \ Man α 1-3 / Man β 1-4GlcNAc β 1-4GlcNAc-PA / Neu5Ac α 2-3Gal β 1-4GlcNAc β 1-2Man α 1-3	0.3	–
pM3-2	11.9 (6.7)	1954	Man α 1-6 \ Fuc α 1-6 \ Man α 1-3 / Man β 1-4GlcNAc β 1-4GlcNAc-PA / Neu5Ac α 2-3Gal β 1-4GlcNAc β 1-2Man α 1-3	0.3	–
hM1	7.6 (7.7)	1970	(Hexose)6(HexNAc)3(NEuAc) 1(PA)1[e]	–	0.2
hM2-2	7.9 (6.8)	2255	(Hexose)4(HexNAc)6(NeuAc)1(PA)1[e]	–	0.15
hM4-1	11.2 (6.4)	1792	Man α 1-6 \ Fuc α 1-6 \ Man β 1-4GlcNAc β 1-4GlcNAc-PA / Neu5Ac α 2-6Gal β 1-4GlcNAc β 1-2Man α 1-3	–	0.1
hM4-2	11.2 (6.7)	2011	Gal β 1-4GlcNAc β 1-2Man α 1-6 \ Man β 1-4GlcNAc β 1-4GlcNAc-PA / Neu5Ac α 2-3Gal β 1-4GlcNAc β 1-2Man α 1-3	–	0.4
pM4 = hM5	13.5 (7.6)	2157	Gal β 1-4GlcNAc β 1-2Man α 1-6 \ Fuc α 1-6 \ Man β 1-4GlcNAc β 1-4GlcNAc-PA / Neu5Ac α 2-6Gal β 1-4GlcNAc β 1-2Man α 1-3	0.5	0.5
pM5	14.4 (6.2)	1995	GlcNAc β 1-2Man α 1-6 \ Fuc α 1-6 \ Man β 1-4GlcNAc β 1-4GlcNAc-PA / Neu5Ac α 2-3Gal β 1-4GlcNAc β 1-2Man α 1-3	0.6	–
M6	15.1 (7.1)	2157	Gal β 1-4GlcNAc β 1-2Man α 1-6 \ Fuc α 1-6 \ Man β 1-4GlcNAc β 1-4GlcNAc-PA / Neu5Ac α 2-3Gal β 1-4GlcNAc β 1-2Man α 1-3	0.6	2.1

[a]Units of GU were calculated from the elution times of the peaks obtained from the ODS column in Figure 2 and the Amide column in Figure 3.
[b]Average mass calculated from the *m/z* values of $[M + Na]^+$ or $[M + H]^+$ ion for neural, $[M - H]^-$ ion for mono-sialyl and mono-sulfated and $[M + Na - 2H]^-$ ions for mono-sialyl-mono-sulfated and di-sulfated PA-oligosaccharides (Supplementary data, Figure S1).
[c]Structures of PA-oligosaccharides are represented.
[d]Molecular percentage of was calculated from the peak area in Figure 2 by comparison with total *N*-glycan content in each islet tissue.
[e]*N*-glycans did not coincide with those of known references in the GALAXY database.

Table III. Structures and relative quantities of neutral, mono-sialyl, di-sialyl or mono-sulfate, mono-sialyl-mono-sulfate and di-sulfate PA-oligosaccharides derived from human and porcine islets

Peak code number	GU[a] ODS (Amid)	Molecular[b] mass (Da)	Structure[c]	Relative quantity (%)[d]	
				Pig	Human
Di-sialyl glycan					
D1	10.6 (7.5)	2302	Neu5Acα2-6Galβ1-4GlcNAcβ1-2Manα1-6 \ Manβ1-4GlcNAcβ1-4GlcNAc-PA / Neu5Acα2-6Galβ1-4GlcNAcβ1-2Manα1-3	0.2	0.4
hD2	12.1 (6.5)	2302	Neu5Acα2-3Galβ1-4GlcNAcβ1-2Manα1-6 \ Manβ1-4GlcNAcβ1-4GlcNAc-PA / Neu5Acα2-3Galβ1-4GlcNAcβ1-2Manα1-3	–	0.3
pD2 = hD3	13.5 (7.9)	2448	Neu5Acα2-6Galβ1-4GlcNAcβ1-2Manα1-6 \ Fucα1-6 \ Manβ1-4GlcNAcβ1-4GlcNAc-PA / Neu5Acα2-6Galβ1-4GlcNAcβ1-2Manα1-3	0.8	0.2
pD3 = hD4	15.8 (6.9)	2448	Neu5Acα2-3Galβ1-4GlcNAcβ1-2Manα1-6 \ Fucα1-6 \ Manβ1-4GlcNAcβ1-4GlcNAc-PA / Neu5Acα2-3Galβ1-4GlcNAcβ1-2Manα1-3	0.5	0.9

[a]Units of GU were calculated from the elution times of the peaks obtained from the ODS column in Figure 2 and the Amide column in Figure 3.
[b]Average mass calculated from the *m/z* values of $[M+Na]^+$ or $[M+H]^+$ ion for neural, $[M-H]^-$ ion for mono-sialyl and mono-sulfated and $[M+Na-2H]^-$ ions for mono-sialyl-mono-sulfated and di-sulfated PA-oligosaccharides (Supplementary data, Figure S1).
[c]Structures of PA-oligosaccharides are represented.
[d]Molecular percentage of was calculated from the peak area in Figure 2 by comparison with total *N*-glycan content in each islet tissue.
[e]*N*-glycans did not coincide with those of known references in the GALAXY database.

Table IV. Structures and relative quantities of neutral, mono-sialyl, di-sialyl or mono-sulfate, mono-sialyl-mono-sulfate and di-sulfate PA-oligosaccharides derived from human and porcine islets

Peak code number	GU[a] ODS (Amid)	Molecular[b] mass (Da)	Structure[c]	Relative quantity (%)[d]	
				Pig	Human
Mono-sulfated glycan					
S1-1	7.3 (3.8)	1478	(Hexose)3(HexNAc)4(HSO3)1(PA)1[e]	0.2	–
S1-2	7.3 (4.5)	1641	SHO3 \ GalNAcβ1-4GlcNAcβ1-2Manα1-3 / Manα1-6 \ Manβ1-4GlcNAcβ1-4GlcNAc-PA	0.6	–

[a]Units of GU were calculated from the elution times of the peaks obtained from the ODS column in Figure 2 and the Amide column in Figure 3.
[b]Average mass calculated from the *m/z* values of $[M+Na]^+$ or $[M+H]^+$ ion for neural, $[M-H]^-$ ion for mono-sialyl and mono-sulfated and $[M+Na-2H]^-$ ions for mono-sialyl-mono-sulfated and di-sulfated PA-oligosaccharides (Supplementary data, Figure S1).
[c]Structures of PA-oligosaccharides are represented.
[d]Molecular percentage of was calculated from the peak area in Figure 2 by comparison with total *N*-glycan content in each islet tissue.
[e]*N*-glycans did not coincide with those of known references in the GALAXY database.

and collected by centrifugation at 400 × *g* for 1 min. The islets were then suspended in 4 mL of 1000 PU/mL Dispase-II (Godo-Shusei Co. Tokyo, Japan) and treated at 37°C for 15 min. Cell aggregates were allowed to settle and the supernatant was transferred to a conical tube. The pooled harvests were centrifuged at 400 × *g* for 3 min. The cell pellet was washed twice with phosphate buffer saline (PBS) and re-suspended in PBS.

Flowcytometry

The islets were incubated with a 10% solution of normal human pooled serum (NHS) at 4°C for 1 h, washed and then incubated with 1.25 μg of fluorescein isothiocynate-conjugated anti-human IgG and IgM (Cappel, West Chester, PA) as a second antibody for 1 h at 4°C. The stained cells were analyzed with a FACS Calibur flow cytometer (Nippon Becton Dickinson, Tokyo, Japan).

Sulfate-depleted cells

Islets were starved for 24 h in sulfate-free RPMI1640 medium containing 1% of fetal cow serum supplemented with fresh 10 mM sodium chlorate (Nakarai Tesque, Kyoto, Japan).

Supplementary data

Supplementary data for this article are available online at http://glycob.oxfordjournals.org/.

Table V. Structures and relative quantities of neutral, mono-sialyl, di-sialyl or mono-sulfate, mono-sialyl-mono-sulfate and di-sulfate PA-oligosaccharides derived from human and porcine islets

Peak code number	GU[a] ODS (Amid)	Molecular[b] mass (Da)	Structure[c]	Relative quantity (%)[d]	
				Pig	Human
Mono-sialyl-mono-sulfated glycan					
MS1	9.8 (5.0)	2133	(Hexose)4(HexNAc)5(NeuAc)1(HSO3)1(PA)1[e]	0.3	–
MS2	12.7 (5.3)	2279	Neu5Acα2-6Galβ1-4GlcNAcβ1-2Manα1-6 (SHO3 / GalNAcβ1-4GlcNAcβ1-2Manα1-3) ; Fucα1-6 ; Manβ1-4GlcNAcβ1-4GlcNAc-PA	1.3	–
MS3	15.9 (5.4)	2279	(Hexose)4(HexNAc)5(Deoxyhexose)1(NeuAc)1(HSO3)1(PA)1*	0.4	–

[a]Units of GU were calculated from the elution times of the peaks obtained from the ODS column in Figure 2 and the Amide column in Figure 3.
[b]Average mass calculated from the *m/z* values of $[M + Na]^+$ or $[M + H]^+$ ion for neural, $[M - H]^-$ ion for mono-sialyl and mono-sulfated and $[M + Na - 2H]^-$ ions for mono-sialyl-mono-sulfated and di-sulfated PA-oligosaccharides (Supplementary data, Figure S1).
[c]Structures of PA-oligosaccharides are represented.
[d]Molecular percentage of was calculated from the peak area in Figure 2 by comparison with total *N*-glycan content in each islet tissue.
[e]*N*-glycans did not coincide with those of known references in the GALAXY database.

Table VI. Structures and relative quantities of neutral, mono-sialyl, di-sialyl or mono-sulfate, mono-sialyl-mono-sulfate and di-sulfate PA-oligosaccharides derived from human and porcine islets

Peak code number	GU[a] ODS (Amid)	Molecular[b] mass (Da)	Structure[c]	Relative quantity (%)[d]	
				Pig	Human
Di-sulfated glycan					
S2	12.7 (3.9)	2110	(SHO3 / GalNAcβ1-4GlcNAcβ1-2Manα1-6) ; (SHO3 / GalNAcβ1-4GlcNAcβ1-2Manα1-3) ; Fucα1-6 ; Manβ1-4GlcNAcβ1-4GlcNAc-PA	7.0	–

[a]Units of GU were calculated from the elution times of the peaks obtained from the ODS column in Figure 2 and the Amide column in Figure 3.
[b]Average mass calculated from the *m/z* values of $[M + Na]^+$ or $[M + H]^+$ ion for neural, $[M - H]^-$ ion for mono-sialyl and mono-sulfated and $[M + Na - 2H]^-$ ions for mono-sialyl-mono-sulfated and di-sulfated PA-oligosaccharides (Supplementary data, Figure S1).
[c]Structures of PA-oligosaccharides are represented.
[d]Molecular percentage of was calculated from the peak area in Figure 2 by comparison with total *N*-glycan content in each islet tissue.
[e]*N*-glycans did not coincide with those of known references in the GALAXY database.

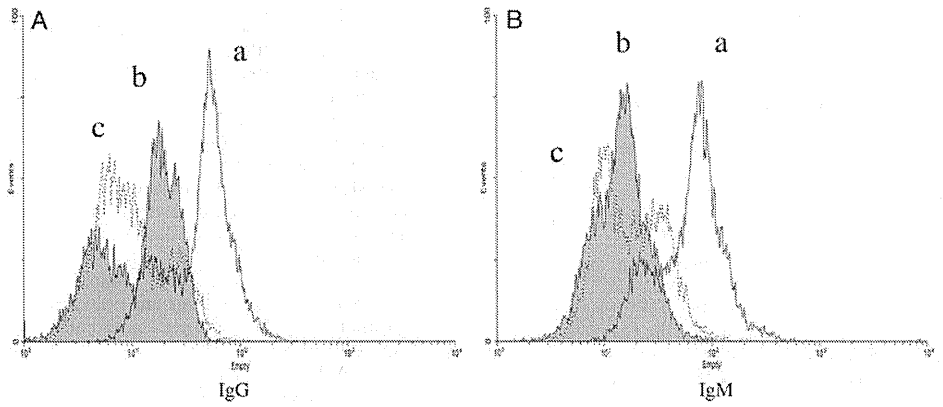

Fig. 8. FACS analysis for the antigenicity of sulfate structures. Islets from adult pigs were treated with 10% NHS as the first antibody and anti-human immmunoglobulins as the second antibodies. Typical FACS profiles of human IgG (**A**) and IgM (**B**) deposition on islets are shown. The effect of removal of sulfate structures by sodium chlorate and sulfate-free medium on the antigenicity of pig islet cells was next investigated. The presence of sodium chlorate led to a reduction in the reactivity of islets to a natural antibody, suggesting that the sulfate structures of islets contain a considerable amount of natural antibody epitopes; a, Normal line: API in usual medium; b, painted out: Sulfate depleted API and c, dotted line: Second antibody control.

Funding

This work was supported by Grants-in Aid for Scientific Research, and Health and Labor Sciences Research Grants, Japan.

Acknowledgements

The authors thank Dr. Milton. S. Feather for his editing of the manuscript and Drs. Akihiro Kondo and Koichi Honke for excellent advice.

Conflict of interest

None declared.

Abbreviations

2D, two dimension; API, adult pig islets; ATP, adenosine triphosphate; DEAE, diethylaminoethyl; FCS, fetal cow serum; FITC, fluorescein isothiocynate; GALAXY, glycoanalysis by the three axes of MS and chromatography; GalNAc, *N*-acetylgalactosamine; GKO, α1-3-galactosyltransferase knockout; GlcNAc, *N*-acetylglucosamine; GU, glucose unit; Hex, hexose; HexNAc, *N*-acetylhexosamine; HPLC, high-performance liquid chromatography; Lew^x, Lewis x; MALDI-TOF-MS, matrix-assisted laser desorption/ionization time-of-flight mass spectrometric; Man, mannose; MS2, mono-sialyl-mono-sulfate; NeuAc, neuranimic acid; NeuGc, N-glycolylneuraminic acid; NHS, normal human pooled serum; ODS, octa decyl silyl; PA, pyridylamino; PBS, phosphate buffer saline; S2, di-sulfate; α-Gal, α-galactosidase.

References

Blixt O, Kumagai-Braesch M, Tibel A, Groth CG, Holgersson J. 2009. Anticarbohydrate antibody repertories in patients transplanted with fetal pig islets revealed by glycan arrays. *Am J Transplant.* 9:83–90.

Boregowda RK, Mi Y, Bu H, Baenziger JU. 2005. Differential expression and enzymatic properties of GalNAc-4-sulfotransferase-1 and GalNAc-4-sulfotransferase-2. *Glycobiology.* 15:1349–1358.

Breimer ME. 2011. Gal/non-Gal antigens in pig tissues and human non-Gal antibodies in the GalT-KO era. *Xenotransplantation.* 18:215–228.

Byrne GW, Stalboerger PG, Du Z, Davis TR, McGregor CG. 2011. Identification of new carbohydrate and membrane protein antigens in cardiac xenotransplantation. *Transplantation.* 91:287–292.

Dai Y, Vaught TD, Boone J, Chen SH, Phelps CJ, Ball S, Monahan JA, Jobst PM, McCreath KJ, Lamborn AE, et al. 2002. Targeted disruption of the alpha1,3-galactosyltransferase gene in cloned pigs. *Nat Biotechnol.* 20:251–255.

Diswall M, Gustafsson A, Holgersson J, Sandrin MS, Breimer ME. 2011. Antigen-binding specificity of anti-αGal reagents determined by solid-phase glycolipid-binding assays. A complete lack of αGal glycolipid reactivity in α1,3GalT-KO pig small intestine. *Xenotransplantation.* 18:28–39.

Elliott RB. 2011. Towards xenotransplantation of pig islets in the clinic. *Curr Opin Organ Transplant.* 16:195–200.

Ezzelarab M, Ayares D, Cooper DK. 2005. Carbohydrates in xenotransplantation. *Immunol Cell Biol.* 83:396–404.

Galili U, Clark MR, Shohet SB, Buehler J, Macher BA. 1987. Evolutionary relationship between the natural anti-Gal antibody and the Gal alpha 1—3Gal epitope in primates. *Proc Natl Acad Sci USA.* 84:1369–1373.

Girard JP, Baekkevold ES, Amalric F. 1998. Sulfation in high endothelial venules:cloning and expression of the human PAPS synthetase. *FASEB J.* 12:603–612.

Goto M, Eich TM, Felldin M, Foss A, Källen R, Salmela K, Tibell A, Tufveson G, Fujimori K, Engkvist M, et al. 2004. Refinement of the automated method for human islet isolation and presentation of a closed system for in vitro islet culture. *Transplantation.* 78:1367–1375.

Kim YG, Gil GC, Harvey DJ, Kim BG. 2008. Structural analysis of alpha-Gal and new non-Gal carbohydrate epitopes from specific pathogen-free miniature pig kidney. *Proteomics.* 8:2596–2610.

Kim YG, Gil GC, Jang KS, Lee S, Kim HI, Kim JS, Chung J, Park CG, Harvey DJ, Kim BG. 2009. Qualitative and quantitative comparison of *N*-glycans between pig endothelial and islet cells by high-performance liquid chromatography and mass spectrometry-based strategy. *J Mass Spectrom.* 44: 1087–1104.

Kim YG, Harvey DJ, Yang YH, Park CG, Kim BG. 2009. Mass spectrometric analysis of the glycosphingolipid-derived glycans from miniature pig endothelial cells and islets: Identification of NeuGc epitope in pig islets. *J Mass Spectrom.* 44:1489–1499.

Kim YG, Kim SY, Hur YM, Joo HS, Chung J, Lee DS, Royle L, Rudd PM, Dwek RA, Harvey DJ, et al. 2006. The identification and characterization of xenoantigenic nonhuman carbohydrate sequences in membrane proteins from porcine kidney. *Proteomics.* 6:1133–1142.

Komoda H, Miyagawa S, Kubo T, Kitano E, Kitamura H, Omori T, Ito T, Matsuda H, Shirakura R. 2004. A study of the xenoantigenicity of adult pig islets cells. *Xenotransplantation.* 11:237–246.

Matsumoto S, Okitsu T, Iwanaga Y, Noguchi H, Nagata H, Yonekawa Y, Yamada Y, Fukuda K, Shibata T, Kasai Y, et al. 2006. Successful islet transplantation from nonheartbeating donor pancreata using modified Ricordi islet isolation method. *Transplantation.* 82:460–465.

Matsumoto S, Qualley SA, Goel S, Hagman DK, Sweet IR, Poitout V, Strong DM, Robertson RP, Reems JA. 2002. Effect of the two-layer (University of Wisconsin solution-perfluorochemical plus O_2) method of pancreas preservation method on human islet isolation, as assessed by the Edmonton isolation protocol. *Transplantation.* 74:1414–1419.

Miyagawa S, Ueno T, Nagashima H, Takama Y, Fukuzawa M. 2012. Carbohydrate antigens. *Curr Opin Organ Transplant.* 17:174–179.

Ono J, Takaki R, Fukuma M. 1977. Preparation of single cells from pancreatic islets of adult rat by the use of dispase. *Endocrinol Jpn.* 24:265–270.

Sriwilaijaroen N, Kondo S, Yagi H, Takemae N, Saito T, Hiramatsu H, Kato K, Suzuki Y. 2011. *N*-glycans from porcine trachea and lung: Predominant NeuAcα2–6Gal could be a selective pressure for influenza variants in favor of human-type receptor. *PLoS One.* 6:e16302.

Takahagi Y, Fujimura T, Miyagawa S, Nagashima H, Shigehisa T, Shirakura R, Murakami H. 2005. Production of alpha 1,3-galactosyltransferase gene knockout pigs expressing both human decay-accelerating factor and *N*-acetylglucosaminyltransferase III. *Mol Reprod Dev.* 71:331–338.

Takahashi N, Kato K. 2003. GALAXY(Glycoanalysis by the three axes of MS and chromatography): A web application that assists structural analyses of *N*-glycans. *Trends Glycosci Glycotech.* 15:235–251.

Takahashi N, Khoo KH, Suzuki N, Johnson JR, Lee YC. 2001. *N*-glycan structures from the major glycoproteins of pigeon egg white: Predominance of terminal Gala(1–4)Gal. *J Biol Chem.* 276:23230–23239.

Thompson P, Badell IR, Lowe M, Cano J, Song M, Leopardi F, Avila J, Ruhil R, Strobert E, Korbutt G, et al. 2011. Islet xenotransplantation using gal-deficient neonatal donors improves engraftment and function. *Am J Transplant.* 11:2593–2602.

Varki A. 2009. Multiple changes in sialic acid biology during human evolution. *Glycoconj J.* 26:231–245.

Wheeler SF, Harvey DJ. 2001. Extension of the in-gel release method for structural analysis of neutral and sialylated *N*-linked glycans to the analysis of sulfated glycans:application to the glycans from bovine thyroid-stimulating hormone. *Anal Biochem.* 296:92–100.

Yagi H, Takahashi N, Yamaguchi Y, Kimura N, Uchimura K, Kannagi R, Kato K. 2005. Development of structural analysis of sulfated N-glycans by multidimensional high performance liquid chromatography mapping methods. *Glycobiology.* 15:1051–1060.

Yamamoto A, Ikeda K, Wang D, Nakatsu S, Takama Y, Ueno T, Nagashima H, Kondo A, Fukuzawa M, Miyagawa S. 2013. Trial using pig cells with the H-D antigen knocked down. *Surg Today.* 43:782–786.

Journal of Reproduction and Development

Accepted for publication: March 11, 2014
Published online: April 21, 2014

Transgenic pigs with pancreas-specific expression of green fluorescent protein

Hitomi MATSUNARI[1,2,3], Toshihiro KOBAYASHI[3,4)*], Masahito WATANABE[1,2)], Kazuhiro UMEYAMA[1,2)], Kazuaki NAKANO[2)], Takahiro KANAI[2)], Taisuke MATSUDA[2)], Masaki NAGAYA[1,2)], Manami HARA[5)], Hiromitsu NAKAUCHI[3, 4)] and Hiroshi NAGASHIMA[1,2,3)]

[1)] Meiji University International Institute for Bio-Resource Research, Kawasaki 214-8571, Japan

[2)] Laboratory of Developmental Engineering, Department of Life Sciences, School of Agriculture, Meiji University, Kawasaki 214-8571, Japan

[3)] Nakauchi Stem Cell and Organ Regeneration Project, ERATO, Japan Science and Technology Agency, Tokyo 102-0075, Japan

[4)] Division of Stem Cell Therapy, Center for Stem Cell Biology and Medicine, Institute of Medical Science, The University of Tokyo, Minato-ku 108-8639, Japan

[5)] Department of Medicine, The University of Chicago, Chicago, IL 60637, USA

*Present address: Wellcome Trust /Cancer Research UK Gurdon Institute, University of Cambridge, Cambridge CB2 1QN, UK

Running head

Pancreas-specific transgene expression

Corresponding Author: Hiroshi Nagashima (hnagas@isc.meiji.ac.jp)

23 **Abstract**

24 The development and regeneration of the pancreas is of considerable interest because of the
25 role of these processes in pancreatic diseases, such as diabetes. Here, we sought to develop a large
26 animal model in which the pancreatic cell lineage could be tracked. The pancreatic and duodenal
27 homeobox-1 (*Pdx1*) gene promoter was conjugated to Venus, a green fluorescent protein, and
28 introduced into 370 *in vitro*-matured porcine oocytes by intracytoplasmic sperm injection-mediated
29 gene transfer. These oocytes were transferred into four recipient gilts, all of which became pregnant.
30 Three gilts were sacrificed at 47-65 days of gestation, and the fourth was allowed to farrow. Seven of
31 16 fetuses obtained were transgenic (Tg) and exhibited pancreas-specific green fluorescence. The
32 fourth recipient gilt produced a litter of six piglets, two of which were Tg. The founder Tg offspring
33 matured normally and produced healthy first-generation (G1) progeny. A postweaning autopsy of four
34 27-day-old G1 Tg piglets confirmed the pancreas-specific Venus expression. Immunostaining of the
35 pancreatic tissue indicated the transgene was expressed in β-cells. Pancreatic islets from Tg pigs were
36 transplanted under the renal capsules of NOD/SCID mice and expressed fluorescence up to one month
37 after transplantation. Tg G1 pigs developed normally and had blood glucose levels within the normal
38 range. Insulin levels before and after sexual maturity were within normal ranges, as were other blood
39 biochemistry parameters, indicating that pancreatic function was normal. We conclude that
40 *Pdx1-Venus* Tg pigs represent a large animal model suitable for research on pancreatic
41 development/regeneration and diabetes.

42

43 **Key words**

44 ICSI-mediated gene transfer, Pancreas generation, Pdx1, Transgenic pig, Venus

45

Introduction

The development and utilization of genetically modified pigs have contributed to the expansion of many biomedical research efforts. For example, genetically modified pigs serving as disease models for retinitis pigmentosa [1], diabetes [2, 3], and cystic fibrosis [4, 5] have been produced, and these models are expected to further the development of new drugs and treatment methods. In xenotransplantation research, α1,3-galactosyltransferase gene knockout pigs and pigs carrying human complement regulatory factor genes have been produced [for review, see 6, 7] and are now being used in preclinical experiments, such as the transplantation of swine organs to monkeys. Additionally, pigs expressing fluorescent proteins are exceptionally useful in research on topics such as cell tracking [8, 9] and tissue regeneration [10]. Even more innovative and more widely applicable research results are likely to be obtained through the future use of genetically modified pigs. The aim of our research was to produce transgenic (Tg) pigs to advance research on pancreas generation.

Overcoming diabetes is a global challenge for modern society; thus, the production of Tg pigs that can be used to understand the mechanisms underlying pancreatic development and the control of pancreatic functions is of great value. We therefore embarked on a program to produce Tg pigs that express the Venus variant of green fluorescent protein (GFP) [11] under the control of the pancreatic duodenal homeobox-1 (*Pdx1*) gene promoter. *Pdx1* functions as a master gene that induces the differentiation of β-cells from pancreatic stem cells, and research on Pdx1-positive cells is important for understanding the development of the pancreas and β-cell differentiation [12, 13]. The study of Pdx1-positive pancreatic stem cells may also lead to improved pathophysiological analysis and the development of treatments [13].

Methods for producing Tg pigs include pronuclear DNA injection [14], somatic cell nuclear transfer [15] and intracytoplasmic sperm injection-mediated gene transfer (ICSI-MGT) [16]. We chose ICSI-MGT for the present study, having previously confirmed that ICSI-MGT to *in vitro*-matured (IVM) porcine oocytes enables the production of Tg pigs with a high potential for reproducibility [2 ,

71 17].

72 In the present study, we first produced several Tg pig fetuses by ICSI-MGT to confirm that the
73 transferred *Pdx1-Venus* gene was expressed exclusively in the pancreas. Then, we produced Tg pigs
74 and examined their progeny to determine whether the genes were transmitted to the succeeding
75 generation, confirming the reproducibility of the pattern of pancreas-specific expression. We further
76 transplanted pancreatic islets of the *Pdx1-Venus* Tg pig to immunodeficient mice to verify their *in vivo*
77 traceability. The utility of the *Pdx1-Venus* Tg pigs as a model for research on pancreatic development
78 is discussed.

79

80

Materials and Methods

Animal care

All animal experiments in this study were approved by the Institutional Animal Care and Use Committee of Meiji University (IACUC-07-0005).

Chemicals

All chemicals were purchased from the Sigma Aldrich Chemical Co. (St. Louis, MO, USA) unless otherwise indicated.

Construction of the Pdx1-Venus transgene

The *Pdx1-Venus* transgene construct (8.4 kb) consisted of the mouse *Pdx1* promoter, *Venus* cDNA, and rabbit β-globin gene sequence (from partway through the second exon to the 3' untranslated region), including a polyadenylation signal (pA) (Fig. 1). The transgene fragment was excised from the plasmid vector by enzymatic digestion using the *Bss*HII restriction enzyme (Takara Bio, Inc., Shiga, Japan), separated by gel electrophoresis, and purified using the QIAquick® Gel Extraction Kit (QIAGEN, Hilden, Germany).

In vitro maturation of oocytes

Porcine ovaries were collected at a local abattoir and transported to the laboratory in Dulbecco's phosphate buffered saline (DPBS, Nissui Pharmaceutical, Tokyo, Japan) containing 75 μg/ml potassium penicillin G, 50 μg/ml streptomycin sulfate, 2.5 μg/ml amphotericin B, and 0.1% (w/v) polyvinyl alcohol (PVA). Cumulus-oocyte complexes were collected from the ovarian antral follicles (3.0 to 6.0 mm in diameter) by aspiration with a 10-ml syringe and a 20 G hypodermic needle, and those with at least three layers of compacted cumulus cells were selected and cultured in NCSU23 medium [18] supplemented with 0.6 mM cysteine, 10 ng/ml epidermal growth factor, 10% (v/v)

106 porcine follicular fluid, 75 μg/ml potassium penicillin G, 50 μg/ml streptomycin sulfate, 10 IU/ml eCG
107 (ASKA Pharmaceutical, Co., Tokyo, Japan), and 10 IU/ml hCG (ASKA Pharmaceutical) at 38.5 C in a
108 humidified atmosphere of 5% CO_2 in air for 22 h. Then, the oocytes were cultured for an additional 21
109 h without eCG and hCG at 38.5 C in a humidified atmosphere of 5% CO_2, 5% O_2, and 90% N_2 [19].
110 IVM oocytes with expanded cumulus cells were treated with 1 mg/ml hyaluronidase dissolved in
111 Tyrode lactose medium containing 10 mM HEPES and 0.3% (w/v) polyvinylpyrrolidone
112 (TL-HEPES-PVP) and separated from the cumulus cells by gentle pipetting. Oocytes with an evenly
113 granulated ooplasm and an extruded first polar body were selected for the subsequent experiments.
114
115 *Porcine sperm preparation for ICSI-MGT*
116 Commercially available boar semen (Duroc) suitable for artificial insemination was used to
117 prepare frozen sperm for ICSI-MGT. Beltsville thawing solution (BTS) was used as a freezing
118 solution without cryoprotective agents [20]. The sperm were washed three times by centrifugation at
119 200 ×g for 5 min in BTS to remove the extender. The sperm were then suspended in BTS (containing
120 5% (w/v) BSA) at a concentration of 3×10^7 cells/ml, placed in 0.25-ml plastic freezing straws
121 (Fujihira Industry Co., Ltd., Tokyo, Japan), and plunged into liquid nitrogen. The straws of frozen
122 sperm were thawed by soaking in a 37 C water bath for 10 sec. The sperm recovered from the straws
123 were washed twice in BTS (containing 0.1% (w/v) BSA), suspended in Nucleus Isolation Medium
124 (NIM) [21], and used in ICSI-MGT within 60 min of thawing. For tail removal by sonication, an
125 ultrasonic sonicator (Honda Electronics Co., Ltd., Aichi, Japan) was used to apply ultrasonic
126 vibrations (100 W, 28 kHz) for 9 sec to 300 μl of the sperm suspension (5×10^7 cells/ml) in a 1.5-ml
127 microcentrifuge tube. This duration of sonication was determined to decapitate approximately 70% of
128 the sperm. Sperm that had been subjected to tail removal by sonication were resuspended in NIM at a
129 concentration of 2-5 $\times 10^4$ cells/μl. Next, the DNA solution was added to the sperm suspension to
130 yield a concentration of 2.5 ng/μl. The suspension was then gently mixed and incubated at room

131 temperature for 5 min. The resulting sperm were stored on ice until use in ICSI-MGT.

132

133 *Intracytoplasmic sperm injection*

134 The IVM oocytes at 43-45 h after commencement of the maturation culture were activated by
135 electrical stimulation before the injection of sperm heads. The oocytes were lined up between two wire
136 electrodes (1.0 mm apart) of a fusion chamber (CUY500G1, Nepa Gene, Chiba, Japan) and overlaid
137 with an activation solution, consisting of 0.28 M mannitol (Nacalai Tesque, Kyoto, Japan), 50 μM
138 $CaCl_2$, 100 μM $MgSO_4$, and 0.01% (w/v) PVA. Activation was induced with one DC pulse of 150
139 V/mm for 100 μsec using an electric pulsing machine (ET-1, Fujihira Industry, Co. Ltd.).

140 ICSI-MGT was performed in a 4-μl drop of TL-HEPES-PVP under mineral oil using an Nikon
141 inverted microscope (TE-300, Nikon, Tokyo, Japan) as described previously [17]. Approximately 1 μl
142 of sperm suspension that had been co-incubated with DNA was transferred to a 2-μl drop of 10%
143 (w/v) PVP (in DPBS; Irvine Scientific, Sales Co., Santa Ana, CA, USA). Sperm heads were aspirated
144 from the PVP drop using an injection pipette and moved to the drop containing the oocytes. An oocyte
145 was first captured by a holding pipette. Next, with the oocyte immobilized with its polar body at either
146 the 6- or 12-o'clock position, a sperm head was injected using the piezo-actuated microinjection unit
147 (PMM-150FU, Prime Tech Ltd., Tsuchiura, Japan) and micromanipulators (MO-202U, Narishige Co.
148 Ltd., Tokyo, Japan). Sperm injection was carried out within 30 min of activation of the oocytes.

149 After ICSI-MGT, embryos to be transferred to recipients were cultured in Porcine Zygote
150 Medium-5 (PZM-5, Research Institute for the Functional Peptides, Yamagata, Japan) for 1-3 days
151 under a humidified atmosphere of 5% CO_2, 5% O_2, and 90% N_2 at 38.5 C.

152

153 *Embryo transfer*

154 Crossbred (Large White/Landrace × Duroc) prepubertal gilts weighing from 100 to 105 kg were
155 used as recipients of the sperm-injected embryos. The gilts were treated with a single intramuscular